Hindawi Publishing Corporation
ISRN Cell Biology
Volume 2013, Article ID 265182, 16 pages
http://dx.doi.org/10.1155/2013/265182

Research Article

Identification of PDZ Domain Containing Proteins Interacting with $Ca_v1.2$ and PMCA4b

Doreen Korb,[1] Priscilla Y. Tng,[1] Vladimir M. Milenkovic,[2] Nadine Reichhart,[2] Olaf Strauss,[2] Oliver Ritter,[3] Tobias Fischer,[1] Peter M. Benz,[1] and Kai Schuh[1]

[1] *Institute of Physiology, University of Wuerzburg, Roentgenring 9, 97070 Wuerzburg, Germany*
[2] *Eye Clinic, University of Regensburg, Franz-Josef-Strauss-Allee 11, 93042 Regensburg, Germany*
[3] *Department of Medicine I, University of Wuerzburg, Oberduerrbacherstraße 4, 97080 Wuerzburg, Germany*

Correspondence should be addressed to Kai Schuh; kai.schuh@uni-wuerzburg.de

Received 30 November 2012; Accepted 25 December 2012

Academic Editors: T. Yazawa, N. Zambrano, and Y. Zhang

Copyright © 2013 Doreen Korb et al. This is an open access article distributed under the Creative Commons Attribution License, which permits unrestricted use, distribution, and reproduction in any medium, provided the original work is properly cited.

PDZ (PSD-95/Disc large/Zonula occludens-1) protein interaction domains bind to cytoplasmic protein C-termini of transmembrane proteins. In order to identify new interaction partners of the voltage-gated L-type Ca^{2+} channel $Ca_v1.2$ and the plasma membrane Ca^{2+} ATPase 4b (PMCA4b), we used PDZ domain arrays probing for 124 PDZ domains. We confirmed this by GST pull-downs and immunoprecipitations. In PDZ arrays, strongest interactions with $Ca_v1.2$ and PMCA4b were found for the PDZ domains of SAP-102, MAST-205, MAGI-1, MAGI-2, MAGI-3, and ZO-1. We observed binding of the $Ca_v1.2$ C-terminus to PDZ domains of NHERF1/2, Mint-2, and CASK. PMCA4b was observed to interact with Mint-2 and its known interactions with Chapsyn-110 and CASK were confirmed. Furthermore, we validated interaction of $Ca_v1.2$ and PMCA4b with NHERF1/2, CASK, MAST-205 and MAGI-3 via immunoprecipitation. We also verified the interaction of $Ca_v1.2$ and nNOS and hypothesized that nNOS overexpression might reduce Ca^{2+} influx through $Ca_v1.2$. To address this, we measured Ca^{2+} currents in HEK 293 cells co-expressing $Ca_v1.2$ and nNOS and observed reduced voltage-dependent $Ca_v1.2$ activation. Taken together, we conclude that $Ca_v1.2$ and PMCA4b bind promiscuously to various PDZ domains, and that our data provides the basis for further investigation of the physiological consequences of these interactions.

1. Introduction

PDZ domains are protein interaction motifs that play a crucial role in cellular signaling and bind specifically to cytoplasmatic carboxyl (C-) terminal sequences of their interacting proteins, which often belong to transmembrane receptor and ion channel families. This motif typically spans 90–100 amino acids and was first found in three polypeptides: the mammalian protein postsynaptic density-95 (PSD-95), the *Drosophila melanogaster* epithelial tumor suppressor protein Discs Large (Dlg), and the mammalian epithelial tight junction protein Zonula occludens-1 (ZO-1) [1–7]. Typical ligands for PDZ domains are the high voltage-activated L-type calcium channel (LTCC) $Ca_v1.2$ and the plasma membrane calcium ATPase (PMCA) 4b, both essential for calcium homeostasis in excitable and nonexcitable cells.

Voltage-gated calcium channels (Ca_v) allow the cellular entry of calcium (Ca^{2+}) ions and initiate muscle excitation-contraction coupling, neurotransmitter release, gene expression, or hormone secretion. $Ca_v1.2$ channels play a major role for the voltage-dependent Ca^{2+} influx. Its overexpression augmented Ca^{2+} influx into cardiomyocytes, thereby increasing cardiac contractile force [8, 9]. Further studies demonstrated the importance of $Ca_v1.2$ in the heart. Homozygous $Ca_v1.2$ knockout mice die before day 14.5 p.c., presumably because L-type channels are indispensable during heart development [10, 11]. Furthermore, mutations in the CACNA1C gene, which codes for the $Ca_v1.2$ subunit, are causative for the Timothy syndrome. This disease is characterized by a multiorgan disorder with serious cardiac defects, sudden death, and other comorbidities [12, 13].

PMCAs extrude Ca^{2+} from the cytoplasm into the extracellular space, and they, as primary ion pumps, are

regarded as essential for long term maintenance of low intracellular Ca^{2+}, which is a prerequisite for subsequent Ca^{2+}-dependent intracellular signaling and spatial changes in Ca^{2+} concentrations [14–16]. Mammalian PMCAs are products of four genes (ATP2B1–ATP2B4), which share 80–90% sequence homology at the amino acid level in human, rat, and mouse [17]. In many cell types, PMCAs are concentrated in caveolae [18–20] that are rich in receptors, signal transducers, effectors, and structural proteins, all of which are important for many signaling pathways and the maintenance of cytoskeletal networks [21, 22]. Differential splicing of PMCA RNA transcripts results in a variety of subtypes of these isoforms. More than 20 splice variants have been identified [17]. The C-termini of the b-splice variants of all PMCA isoforms is supposed to bind preferentially to type 1 PDZ domains. The human ETSV* motif of the PMCA4b interacts with members of the membrane-associated guanylate kinase (MAGUK) family [17, 18], such as PSD-95/SAP90, SAP97/hDlg, SAP-102, PSD-93/Chapsyn-110 [18], and calcium/calmodulin-dependent serine protein kinase (CASK) [23], which contain one to six PDZ domains [24, 25]. MAGUKs are essential for organizing signaling complexes, and membrane protein trafficking [26]. PMCA4b interacts with PMCA-interacting single PDZ protein (PISP) [27], Na^+/H^+ exchanger regulatory factor 2 (NHERF2) [28], and neuronal nitric oxide synthase (nNOS), thereby regulating enzyme activity [29]. Besides C-terminal mediated interactions, PMCA4b also interacts with other proteins via other domains, for example, via the second intracellular loop with the tumor suppressor Ras-associated factor 1, calcineurin, and α1-syntrophin [30–32]. So far, there are only few studies about the proteins that may possibly interact with $Ca_v1.2$. To gain more insight into the participating pathways, and the physiological roles of $Ca_v1.2$ and PMCA4b, we searched for new interaction partners. In this study, we show that the $Ca_v1.2$ motif (VSNL*) interacts with the MAGUK protein CASK, and the membrane-associated guanylate kinase-inverted proteins 1, 2, 3 (MAGI-1, MAGI-2, MAGI-3), a subfamily of MAGUK proteins. MAGI-1, MAGI-2, MAGI-3 are also new interaction partners of PMCA4b. Interestingly, we discovered additional proteins that interact with $Ca_v1.2$ as well as with PMCA4b. These are the microtubule-associated testis specific serine/threonine kinase (MAST-205), the tight junction protein Zonula occludens 1 (ZO-1), Rho guanine exchange factor 11 and 12 (GEF11, GEF12), and Mint-2. In addition, we confirmed the lack of PMCA4b interactions with NHERF1 and NHERF2, and in contrast, the binding of $Ca_v1.2$ to the PDZ domain of NHERF1/2. We further showed that the nNOS interacts with $Ca_v1.2$, thereby influencing transmembrane calcium currents.

Our results provide the basis for more detailed analyses of PMCA4b and Ca_v channel regulation, specifically in dependence of the associated PDZ domain containing proteins.

2. Materials and Methods

2.1. Plasmid Constructs. Plasmids encoding Histidine (His)-tagged carboxyl termini of $Ca_v1.2\alpha$ (LTCC) and PMCA4b were made by standard molecular biology techniques. Codons for the final 10 ($Ca_v1.2\alpha$) or 15 (PMCA4b) amino acids were cloned as PstI-XbaI fragments into the pEXP vector (containing a 6xHis tag, Panomics, Fremont, CA, USA) to produce His-tagged fusion proteins (pEXP-$Ca_v1.2\alpha$ and pEXP-PMCA4b) for PDZ Domain Arrays (Panomics). The same codons of LTCC were inserted into the pGEX-4T-3 (GE Healthcare Bio-Sciences AB, Uppsala) vector to produce Glutathion-S-Transferase (GST) fusion proteins (pGEX-4T-3-LTCC). The expression constructs pGEX-4T-1-nNOS-PDZ and pcDNA3-nNOS were kind gifts from David Bredt (University of California, San Francisco, CA). The plasmids pRK5-kinase-MAST205 and pRK5-kinase-PDZ-MAST205 were kind gifts from Rafael Pulido (Centro de Investigacion Principe Felipe, Valencia, Spain) and the plasmid pcDNA3-$Ca_v1.2\alpha$ was a gift from Sebastian Maier (University of Wuerzburg, Germany).

2.2. TranSignal PDZ Domain Array. Plasmid constructs pEXP-$Ca_v1.2\alpha$ and pEXP-PMCA4b were transformed into *E. coli* BL21 (DE3) bacteria, which were then inoculated in 3 mL of LB/Amp (100 μg/mL) and shaken for an hour at 37°C at 300 rpm. After reaching an OD_{600} of 0.5–0.8, 1 mM isopropyl-1-thio-β-D-galactopyranoside (IPTG) was added to the bacteria before further growth for 3-4 h at 37°C to induce target protein expression. Cells were collected by centrifugation (4,000 ×g, 10 min 4°C), resuspended in 2 mL resuspension buffer (Panomics), and lysed with a sonicator. After clearing at 14,000 rpm for 5 min at 4°C, protein content of the supernatant was quantified via bicinchoninic acid (BCA) protein assay. The PDZ Domain Arrays were prepared according to the manufacturer's instructions, incubated with diluted bacterial extract (5 μg/mL in blocking buffer) containing the His-tagged fusion proteins for 1-2 h at room temperature, and washed thrice with wash buffer for 5 min. They were then incubated with 1x Anti-Histidine horse radish peroxidise (HRP) conjugate (Panomics), diluted in wash buffer, for 1-2 h at room temperature. Antibody complexes were detected by enhanced chemiluminescence, using ECL Western blotting substrate (ECL Plus, GE Healthcare). X-rays were scanned and the signals were quantified with ImageJ. The values were standardized against the GST negative control.

2.3. Purification of GST Fusion Proteins. GST and GST fusion proteins were expressed in *E. coli* BL21(DE3) by induction with 1 mM IPTG for 6 h. Bacterial cells were pelleted, resuspended in PBS (137 mM NaCl, 2.7 mM KCl, 100 mM Na_2HPO_4, 2 mM KH_2PO_4, and pH 7.4) containing protease inhibitor (complete EDTA-free Protease Inhibitor Cocktail Tablets, Roche), and lysed by addition of lysozyme (1 mg/mL) and sonication. The lysate was cleared by centrifugation at 30,000 g for 20 min at 4°C. The pellet was resuspended in PBS and the resulting lysate was incubated with Glutathione-Sepharose (GE Healthcare) at constant rotation for 2 h at 4°C. The quantity of the washed and bound fusion proteins was estimated by Coomassie Blue staining of SDS-polyacrylamide gels.

2.4. GST Pull-Down Assays. To prepare tissue lysates, organs were removed from mice and immediately homogenized in cold RIPA buffer (50 mM Tris-HCl, pH 8.0, 150 mM NaCl, 1% Nonidet P-40, 0.5% Na-Deoxycholate, protease inhibitor, and optional 0.1% SDS). The homogenate was centrifuged at 4,000 ×g for 3 min. For cell lysates, the same RIPA buffer was used. 500 μg of each supernatant and 3 μg of bound GST or GST fusion proteins on agarose beads were rotated overnight at 4°C. The beads were pelleted and washed three times in PBS with protease inhibitors. Bound proteins were eluated in 2x Laemmli buffer (4% SDS, 20% glycerol, 10% 2-mercaptoethanol, 0,004% bromphenol blue, 0,125 M Tris HCl, and pH 6.8) [33] and separated on polyacrylamide gels followed by transfer onto nitrocellulose. Nitrocellulose membranes were blocked in TBST (TBS + 0.1% Tween) with 5% milk and incubated with primary and secondary antibodies. HRP-coupled secondary antibodies were detected using ECL Plus.

2.5. Coimmunoprecipitations. HEK 293 cells (DMEM supplemented with 10% FCS), ECV cells (DMEM supplemented with 10% FCS, 4.5 g/L glucose), and HEK 293 cells stably expressing α_{1b} ($Ca_v1.2b$) and the $Ca_v\beta 2a$ subunit of the smooth muscle L-type calcium channel [34, 35] (a gift from Andrea Welling, TU Munich, Germany) (DMEM supplemented with 10% FCS, 200 μg/mL G418 plus 100 μg/mL hygromycin B) were grown to ~80% confluence. Cells were transfected using Lipofectamine 2000 (Invitrogen) according to the manufacturer's instructions. After ~48 h, cells were rinsed with PBS and lysed in RIPA buffer without SDS. Subsequent to 10 min incubation on ice, cells were scraped from the plates and pelleted at 13,000 ×g for 10 min at 4°C. 300 μg of the lysate was used for each immunoprecipitation. 1–5 μg of antibodies: anti-$Ca_v1.2$ (Alomone Labs), anti-MAGI-3 (Abcam), anti-HA (Covance), and anti-PMCA4-JA9 (Sigma) were added, accordingly. After 2 h rocking at 4°C, 50 μL of protein A/G-agarose was added to the mixtures and rotated overnight at 4°C. In all immunoprecipitations, the positive controls were inputs of the respective protein and the negative controls were the relevant protein samples incubated with protein A/G-agarose beads and irrelevant antibodies (anti-AT_2). Protein A/G-agarose was pelleted at 4,000 ×g for 30 s and washed twice with RIPA buffer containing protease inhibitors. Bound proteins were eluated in 2x Laemmli buffer and separated on polyacrylamide gels followed by transfer onto nitrocellulose for Western blotting as described above.

2.6. Antibodies for Immunoblotting. The following antibodies were used for immunoblotting: anti-ZO-1 (BD Transduction Laboratories) used at 1 : 1000 dilution, anti-nNOS (Zymed Laboratories) used at 1 : 2000 dilution, anti-$Ca_v1.2$ (Alomone Labs) diluted 1 : 200, anti-CASK (BD Transduction) diluted 1 : 1000, anti-NHERF1 (Cell Signaling) diluted 1 : 1000, anti-MAGI-3 (Abcam) diluted 1 : 1000, and anti-HA (Covance) diluted 1 : 1000. Secondary goat anti-mouse antibodies were purchased from Jackson Immuno Research and used at 1 : 5000 dilution, goat anti-rabbit (Jackson Immuno Research) used at 1 : 10000 dilution. From eBioscience we used rabbit IgG TrueBlot (diluted 1 : 1000) and mouse IgG TrueBlot (diluted 1 : 1000).

2.7. Immunohistochemistry. Rat hearts embedded in Tissue-Tek (Sakura) were frozen in liquid nitrogen, and cryosections (20 μm) were prepared. Cryosections were placed on glass slides, fixed in 4% paraformaldehyde/PBS for 10 min, permeabilized with 0.2% TritonX-100/PBS for 20 min, and blocked with 5% goat serum in PBS for 1 h to reduce nonspecific binding. Sections were incubated with primary antibodies overnight at 4°C, washed thrice in PBS, followed by incubation with the appropriate secondary antibodies. Stained sections were washed three times in PBS and mounted in Mowiol. The following antibodies were used: polyclonal rabbit anti-$Ca_v1.2$-ATTO 488 (Alomone Labs), polyclonal rabbit anti-NHERF1 (Cell Signaling), polyclonal rabbit anti-MAGI-3 (Abcam), monoclonal mouse anti-PMCA 5F10 (Sigma) and Alexa Fluor 488 goat anti-mouse, and Alexa Fluor 594 goat anti-rabbit (Invitrogen). As controls, the secondary Alexa Fluor-labelled antibodies were used alone. Confocal micrographs were obtained with an Eclipse E600 Nikon microscope using a C1 confocal scanning head and a 60-fold oil immersion objective.

2.8. Tricine-SDS-PAGE. To separate low molecular weight proteins, we used the following reagents: anode buffer (0.2 M Tris, pH 8.0), cathode buffer (0.1 M Tris, 0.1 M Tricine (Sigma Aldrich), 0.1% SDS, and pH 8.25), gel buffer (3.0 M Tris, 0.3% SDS, and pH 8.45), separating gel monomer 16,5 : 1 (49.5% T 6% C) and stacking gel monomer 33 : 1 (49.5% T 3% C), whereas T denotes the total percentage of acrylamide and bisacrylamide (Roth) and C the percentage of the crosslinker relative to the total concentration T [36]. Separating gel solution (16.5% T 6% C) was first prepared by mixing 10 mL separating gel monomer, 10 mL gel buffer, and 3.2 mL glycerol (Merck). For the stacking gel (4% T 3% C), we used 1 mL stacking gel monomer, 3.1 mL gel buffer, and 8.4 mL H_2O. We then added 100 μL APS (Sigma Aldrich) and 10 μL TEMED (Sigma Aldrich) to both gel mixtures. After addition of cathode and anode buffer, electrophoresis was performed at 4°C at 30 V and 200 mA. After entering the stacking gel, the conditions were set to 90 V and 300 mA for 5 h. Gels were subsequently stained with Coomassie Brilliant Blue G250 (Merck).

2.9. Patch-Clamp Recordings. For patch-clamp experiments, HEK 293 cells were transiently transfected with either GFP alone or nNOS and GFP. Transfections were carried out as described above. Cells were analyzed 36 h after transfection. Membrane currents were measured in the whole-cell configuration of the patch-clamp technique. During the recordings, transfected cells were superfused by a bath solution containing NaCl 82 mM, TEA-Cl 20 mM, $BaCl_2$ 30 mM, CsCl 5.4 mM, $MgCl_2$ 1 mM, EGTA 0.1 mM, glucose 10 mM, HEPES 5 mM, pH 7.4 adjusted with NaOH; 302.9 mOsm. The perfusion chamber was mounted onto a stage of an inverted fluorescence microscope. Transfected cells were selected by GFP fluorescence. For whole-cell recording, patch pipettes of

3–5 MΩ were made from borosilicate tubes using a DMZ-Universal Puller (Zeitz). Pipettes were filled with a pipette solution containing CsCl 102 mM, TEA-Cl 10 mM, EGTA 10 mM, $MgCl_2$ 1 mM, Na_2ATP 3 mM, HEPES 5 mM, pH 7.4, adjusted with CsOH; 248 mOsm. Membrane currents were recorded using an EPC-10 computer-controlled patch-clamp amplifier in conjunction with the software TIDA for data acquisition and analysis. The access resistance was compensated for values lower than 10 MΩ. For analysis of voltage-dependent activation, steady-state currents were plotted against the membrane potentials of the electrical stimulation. Plots of each individual cell were fitted using the Boltzmann equation. Statistical significance was tested using one-way analysis of variance (ANOVA). All data were given as mean ± SEM. n = number of independent experiments; * = statistical significance with $P < 0.05$. Mean values of data obtained from Boltzmann fits were calculated for each individual cell.

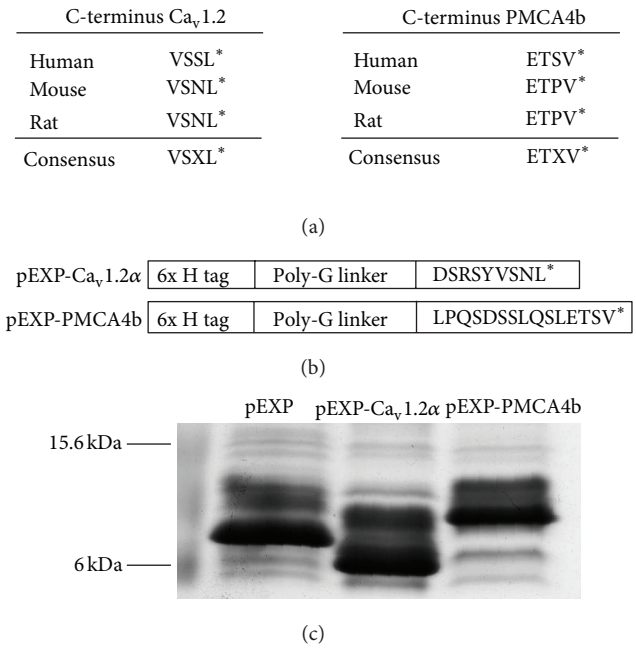

Figure 1: Expression of PDZ array ligands $Ca_v1.2\alpha$ and PMCA4b. (C-terminal ligands for class I PDZ domains). (a) Determination of C-terminal consensus sequence mammalian $Ca_v1.2$ and PMCA4b (b) The final 10 amino acid residues of $Ca_v1.2\alpha$ and the last 15 amino acid residues of PMCA4b were expressed with a 6xHistidine tag linked by a poly-Glycine linker through insertion into the expression vector pEXP. $Ca_v1.2\alpha$ (VSNL*) and PMCA4b (ETSV*), * = stop, possess different C-terminal ends and resulting in interactions with different PDZ domain containing proteins. (c) Tricine-SDS-PAGE to verify the expression of recombinant protein ligands in BL21 bacteria. The shifts between the lanes pEXP (~9 kDa), pEXP-$Ca_v1.2\alpha$ (8.47 kDa), and pEXP-PMCA4b (8.97 kDa), where the read-through product, pEXP, is larger than the PDZ ligands, confirmed their successful expression. Each lane contained 4 μL of bacterial lysate.

3. Results

3.1. Expression of PDZ Array Ligands and PDZ Domain Arrays I-IV. After comparison of C-terminal ends of mammalian $Ca_v1.2$ and PMCA4b (Figure 1(a)), the nucleotide sequences coding for the C-termini were cloned into pEXP bacterial expression vectors (Figure 1(b)). Verification of expression and size of His-tagged recombinant proteins in bacteria via Tricine gel analysis confirmed high expression levels and expected sizes of proteins, that is, for the pEXP read-through, pEXP-$Ca_v1.2\alpha$ and pEXP-PMCA4b, 9 kDa, 8.47 kDa, and 8.97 kDa, as calculated, respectively (Figure 1(c)). Probing the PDZ Domain Arrays with these bacterial lysates and subsequent detection of interactions with anti-6xHis antibodies revealed a series of positive spots on all PDZ arrays tested. As an example, typical results are displayed in Figure 2. Figure 2(a) gives an overview of the arrangement of the PDZ Domain Array III, and the corresponding results for $Ca_v1.2$ and PMCA4b are shown in Figures 2(b) and 2(c), respectively. Subsequent ImageJ quantifications of all four PDZ arrays tested are listed in the Supplemental Tables 1–4 in Supplementary Material available online at http://dx.doi.org/10.1155/2013/265182. The exemplary PDZ Domain Array III was spotted with PDZ domains of scaffolding proteins, especially MAGUKs. ImageJ quantification (Supplemental Table 1) revealed that both ligands interacted strongly with PDZ domains of MAGI-1, MAGI-2, and MAGI-3, and PDZ domains of SCRIB1, and TIP1.

Incubation of the PDZ Domain Array I, on which mainly PDZ domains of synaptic proteins were spotted (overview in Supplemental Figure 1(A)), with the C-terminal PDZ ligands of $Ca_v1.2\alpha$ and PMCA4b, revealed a panel of additional positive PDZ spots, representing possible interaction partners of the $Ca_v1.2\alpha$ and the PMCA4b (Supplemental Figures 1(B) and 1(C)). ImageJ analysis of these signal intensities is listed in Supplemental Table 2. In this case, the $Ca_v1.2\alpha$ and PMCA4b C-termini interacted strongly with the PDZ domains of Mint-2-D1, OMP25, and Dlg-D1, and weakly with CASK-PDZ. In addition to these bindings, a promiscuous binding of the $Ca_v1.2\alpha$ C-terminus to HtrA2, hCLIM1, hPTP1E-D1, RIL, and ZO-2-D3 was detected. Besides the binding of the PMCA4b C-terminus to the PDZ domains of Mint-2-D1, OMP25, Dlg-D1, and CASK, the interaction with the Dlg PDZ domain 2 was very prominent and the signal strength was far above that of the positive controls.

The PDZ Domain Array II is arranged as shown in Supplemental Figure 2(a) and includes some tight junction proteins, sodium/hydrogen exchanger proteins, and other PDZ domains. Strong interactions for both PDZ ligands were observed for ZO-1-D1 and MAST-205 and for the PDZ positive controls (SAP-102). $Ca_v1.2\alpha$ C-terminus also had a high affinity for 4 other PDZ domains: ZO-1-D2, NHERF1-D1, NHERF2-D1/D2, some KIAA proteins, and nNOS (Supplemental Figures 2(B) and 2(C), analyses of signal intensities summarized in Supplemental Table 3).

Probing the PDZ Domain Array IV, mainly consisting of an assortment of scaffolding proteins, MAGUKs, Lin-7 proteins, nucleotide exchange factors, and syntrophins (Supplemental Figure 3(A)), revealed strong interaction of the PMCA4b C-terminus with PDZ domains of MUPP1,

MAGI3 D2	MAGI3 D4	MAGI3 D5	MAGI3 D6	MAGI1 D2	MAGI1 D3	MAGI1 D4	MAGI1 D1	pos	A
MAGI1 D6	MAGI2 D2	MAGI2 D3	MAGI2 D4	MAGI2 D5	MAGI2 D6	hPTP1E D2	hPTP1E D3	pos	B
hPTP1E D4	PTPN4	GRIP1 D4	GRIP1 D3	GRIP1 D2	SCRIB1 D1	SCRIB1 D2	SCRIB1 D4	pos	C
PARD3 D2	PARD3 D3	HARM D3	MLL4	TIP1	SDB2 D2			pos	D
PDZ-pos	GST							pos	E
pos	pos	pos	pos	pos	pos	pos	pos	pos	F
1 2	3 4	5 6	7 8	9 10	11 12	13 14	15 16	17 18	

(a)

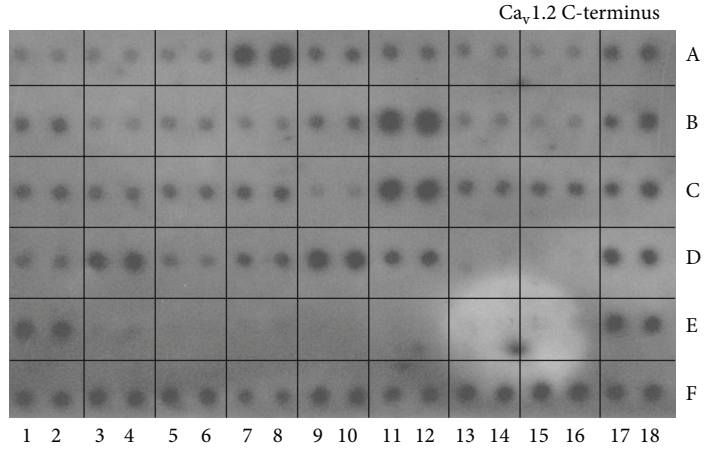

(b)

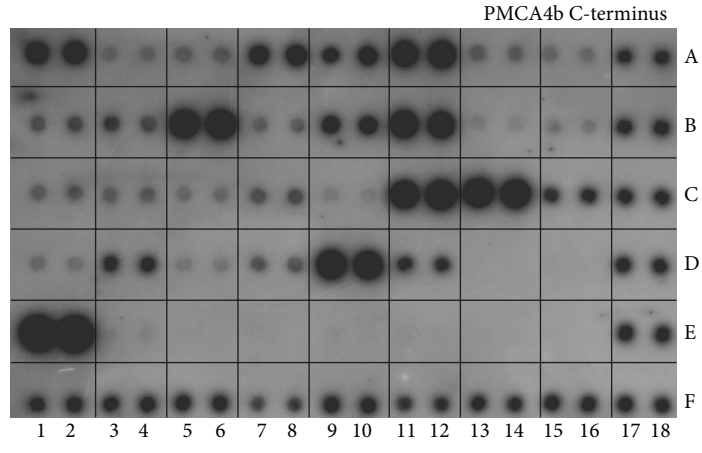

(c)

Figure 2: PDZ Domain Array III. (a) Schematic representation of the TranSignal PDZ Domain Array III. 100 ng of the PDZ domain containing proteins are spotted in duplicate on the array. Pos: positive control (Histidine-tagged ligand), negative control-Glutathione-S-Transferase (GST). (b) PDZ Domain Array III was incubated with the bacterial lysate containing the Histidine-tagged recombinant protein, pEXP-$Ca_v1.2\alpha$. (c) PDZ Domain Array III was incubated with the bacterial lysate containing the Histidine-tagged recombinant protein, pEXP-PMCA4b. Both bacterial extracts had a concentration of 5 μg/mL. PDZ domain and ligand interactions were visualized with anti-Histidine antibodies.

Dlg2 (Chapsyn-110), Dlg3 (SAP-102), LIN7A, LIN7B, LIN7C, SNA1, and SNB1. Both PDZ ligands interact with the PDZ domains of GEF11, GEF12, and SHK1, and the $Ca_v1.2\alpha$ C-terminus binds to that of PIST (results in Supplemental Figures 3(B) and 3(C) and initial quantification of dot intensities summarized in Supplemental Table 4).

For further analyses, some of already established and some of newly identified interaction partners were selected (listed in Table 1), and the interactions were verified in coimmunoprecipitation and colocalization experiments.

3.2. Coimmunoprecipitations of $Ca_v1.2\alpha$ with Putative Interaction Partners. The interaction of $Ca_v1.2\alpha$ with different members of MAGUKs (CASK, MAGI-3, and ZO-1) and the proteins NHERF1 and MAST-205 was verified by coimmunoprecipitations. CASK, a 112 kDa protein, is expressed at neuronal synapses, where it interacts with neurexin, and in renal epithelial cells [37]. Therefore, we examined the putative interaction between $Ca_v1.2\alpha$ and CASK in lysates of HEK 293 cells, which were transfected with $Ca_v1.2\alpha$. Coimmunoprecipitation of CASK with an anti-$Ca_v1.2\alpha$ antibody was further indicative for an interaction of the proteins (Figure 3(a)).

NHERF1, also known as Ezrin binding protein 50, is a 55 kDa phosphoprotein containing two PDZ domains [38]. To test for interaction of full-length proteins, HEK 293 cells, stably expressing the α and the β subunits of $Ca_v1.2$, were subsequently transfected with NHERF1 and coimmunoprecipitations using lysates of these cells were performed. NHERF1 was also coprecipitated with the $Ca_v1.2$-specific antibody in transfected cells (Figure 3(b)).

MAGI-3 (160 kDa) is predominantly expressed in brain but also in other organs [39–41]. Similar to CASK and NHERF1, coimmunoprecipitations revealed interaction of $Ca_v1.2\alpha$ and MAGI-3 in mouse brain lysates (Figure 3(c)).

The tight junction protein ZO-1 is expressed in epithelial and, to a lesser extent, also in endothelial cells [42, 43]. Therefore, we searched for an interaction between $Ca_v1.2\alpha$ and ZO-1 in $Ca_v1.2$-transfected endothelial ECV cells. As depicted in Figure 3(d), the prominent band suggested a robust interaction of $Ca_v1.2\alpha$ and ZO-1 in ECV cells.

The serine/threonine kinase (Ser/Thr kinase) MAST-205 is expressed in testis, brain, and kidney tissues [44, 45]. To test for protein interactions between $Ca_v1.2\alpha$ and MAST-205, we used the HA-tag constructs pRK5-kinase-MAST-205 (36 kDa) and pRK5-kinase-PDZ-MAST-205 (77 kDa), precipitated with the $Ca_v1.2$ specific antibody, and detected the signal with a HA-specific antibody. In this case, the kinase domain alone (third lane) and also the PDZ-containing construct were coprecipitated (Figure 3(e)).

3.3. Coimmunoprecipitations of PMCA4b with Putative Interaction Partners. To confirm our data from the PDZ arrays, we tested for interaction between PMCA4b and CASK by coimmunoprecipitations from kidney and brain lysates, and transfected HEK 293 cells (Figure 4(a)). The results confirmed interaction of PMCA4b and CASK, as previously demonstrated [23]. Binding of the proteins PMCA4b and ZO-1 was demonstrated in extracts from various sources. The PMCA-specific antibody coprecipitated the 220 kDa protein ZO-1 in all cell lysates tested (Figure 4(b)). In both immunoblots, the positive controls were inputs of PMCA4b-transfected HEK 293 cells and the negative controls were the positive controls incubated with A/G-agarose and an irrelevant antibody (anti-AT_2).

3.4. Colocalization of $Ca_v1.2$ and NHERF1, $Ca_v1.2$ and MAGI-3, and PMCA4b and MAGI-3 in Rat Cardiac Myocytes. Confocal laser scanning microscopy studies of rat heart sections revealed localization of $Ca_v1.2$, NHERF1, and MAGI-3 at intercalated discs (Figures 5(a)–5(f)). $Ca_v1.2$ and MAGI-3 were additionally expressed at the transverse tubules (Figures 5(d)–5(f)). As shown in Figures 5(g)–5(i), PMCA4b and MAGI-3 were partially but not completely colocalized at the plasma membrane and the transverse tubules of rat cardiac myocytes.

3.5. Confirmation of Interaction of $Ca_v1.2\alpha$ with the PDZ Domain Containing Protein nNOS by GST Pull-Downs and Coimmunoprecipitation. It has been previously reported that the PDZ domain of nNOS interacts with the C-terminal end of PMCA4b [29]. The Domain Array II (Supplemental Figure 2) indicated that the PDZ domain of nNOS may also interact with $Ca_v1.2\alpha$. To assess this interaction in more detail, we used affinity-purified GST fusion proteins containing the C-terminus of $Ca_v1.2\alpha$ (encoded by the plasmid pGEX-4T-3-LTCC), and the PDZ domain of nNOS (plasmid pGEX-4T-1-nNOS-PDZ). We performed pull-down assays from mouse brain and aorta extracts, and HEK 293 cell lysates, either nontransfected, or transfected with pcDNA3-$Ca_v1.2\alpha$ or pcDNA3-nNOS. As shown in Figure 6(b), the resulting GST pull-down clearly demonstrated binding between the C-terminus of $Ca_v1.2\alpha$ and the nNOS. This interaction was ascertained in reverse, confirming the interaction of nNOS and $Ca_v1.2\alpha$ (Figure 6(a)). Additionally, using an independent assay, we could prove this protein-protein interaction by conventional coimmunoprecipitations. In this assay, we cotransfected HEK 293 cells with the α and β subunits of $Ca_v1.2$ and nNOS. Subsequent precipitation with $Ca_v1.2\alpha$-specific antibodies pulled down nNOS as well (Figure 6(c)).

3.6. Electrophysiological Properties. To examine the electrophysiological properties with $Ca_v1.2$ subunits, Ba^{2+} currents were measured in the whole-cell configuration of the patch-clamp technique. To activate voltage-dependent Ca^{2+} channels, membrane potentials of cells were clamped at a holding potential of −70 mV. From this holding potential the cells were depolarized stepwise in 9 voltage steps of +10 mV increment and a duration of 50 ms to depolarize the cell (Figure 7(a)). HEK cells, which stably express the $Ca_v1.2$ subunit, showed voltage-dependent inwardly directed Ba^{2+} currents with a fast time-dependent activation without inactivation (Figure 7(b)). The kinetic behavior of the $Ca_v1.2$ currents did not change when the cells were additionally transfected with pcDNA3-nNOS (Figure 7(c)). No differences in the overall activity of the currents were detected; $Ca_v1.2$ currents under control conditions but in the presence of nNOS showed no

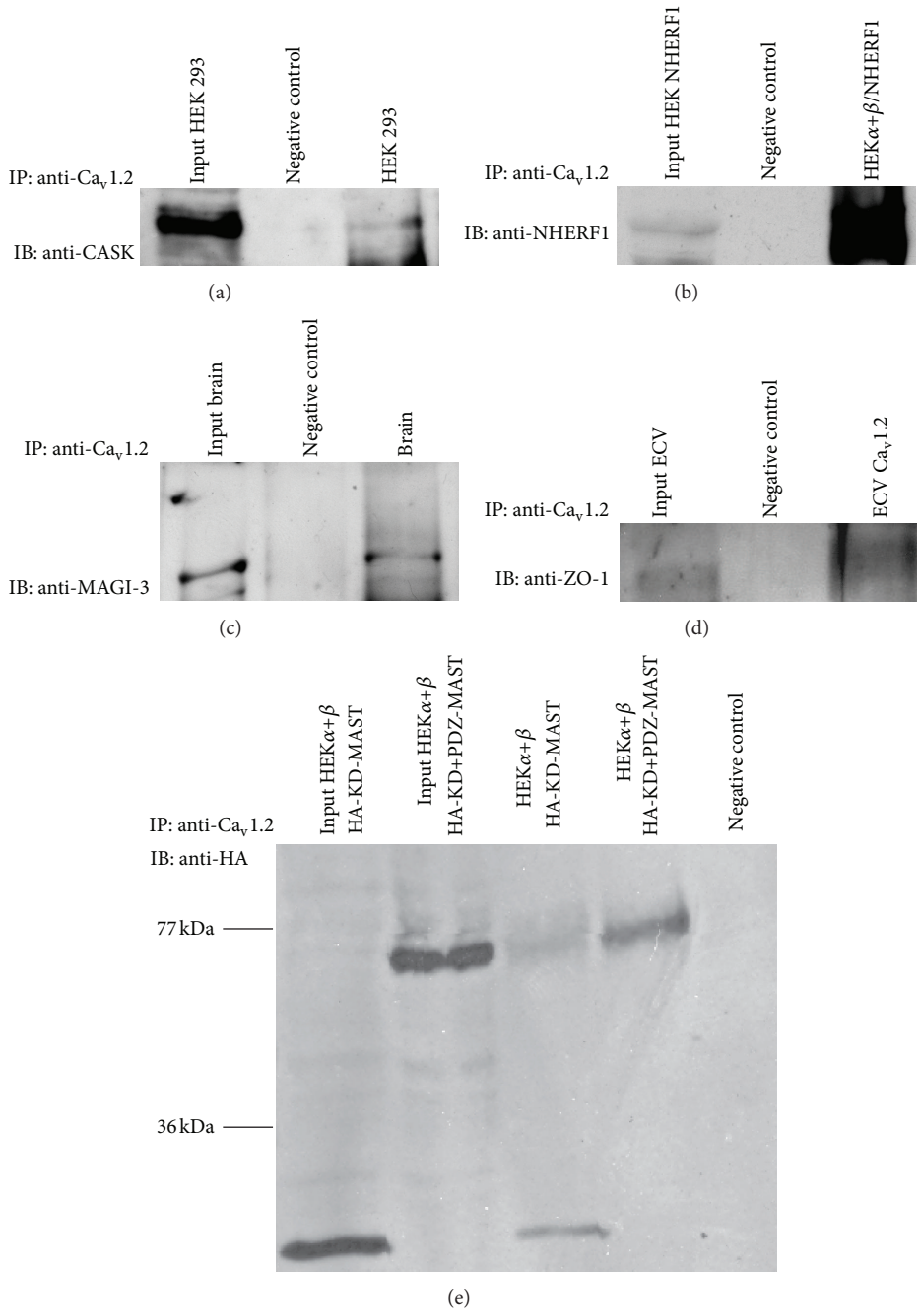

Figure 3: Coimmunoprecipitation of $Ca_v1.2\alpha$. (a) Coimmunoprecipitation demonstrating an interaction of $Ca_v1.2\alpha$ with CASK; CASK was expressed in HEK 293 cells, which we additionally transfected with pcDNA3-$Ca_v1.2\alpha$. We also probed mouse brain lysates. These lysates were precipitated with polyclonal α-$Ca_v1.2$ antibody and probed with monoclonal α-CASK antibody during immunoblotting (IB). The positive control (input) consisted of 20 μg of the HEK 293 lysate. The negative control was HEK 293 cells immunoprecipitated (IP) with an irrelevant antibody (α-NFATc2). (b) Interaction between $Ca_v1.2$ and NHERF1. The positive control was HEK 293 cells transfected with pcDNA3-NHERF1, and the negative control was incubated with an irrelevant antibody (α-AT2). We precipitated HEK 293 cells stably expressing NHERF1 with polyclonal α-$Ca_v1.2$ antibody, and also tissue lysates of heart and kidney. For IB we used α-NHERF1 antibody. (c) IP demonstrated an interaction of $Ca_v1.2\alpha$ with MAGI-3. Positive and negative controls are as described above. $Ca_v1.2\alpha$ antibody was used for IP and MAGI-3 antibody for IB. (d) Interaction between $Ca_v1.2\alpha$ and ZO-1. ZO-1 protein is expressed in ECV cells, hence the positive control was nontransfected ECV cells; the negative control contained ECV cells immunoprecipitated with an irrelevant antibody (α-NFATc2), and for the IP we used $Ca_v1.2$ antibody for precipitation and α-ZO-1 for the IB. (e) HEK 293 cells with stable overexpression of α and β subunits of $Ca_v1.2$ transfected with HA-KD (36 kDa) or HA-KD+PDZ domain of MAST-205 (77 kDa) were incubated with α-$Ca_v1.2$ and protein complexes were subsequently precipitated with protein A/G beads. Western blots were probed with HA antibodies. Irrelevant antibodies were used in negative controls and nonprecipitated organ lysates as positive controls.

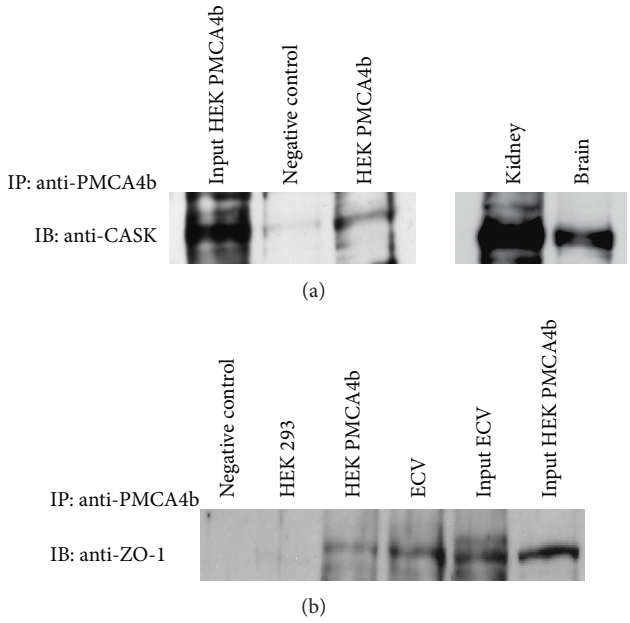

Figure 4: Coimmunoprecipitation of PMCA4b. (a) Lysates of transfected HEK 293-PMCA4b cells, kidney, and brain were incubated with monoclonal antibody specific for PMCA4b (for details see Section 2). Protein complexes were then precipitated with protein A/G beads. Western blot of precipitated proteins were probed with a CASK specific antibody. Irrelevant antibodies were used in negative control (α-NFATc2), and transfected HEK 293-PMCA4b cells were used as positive control. (b) Coimmunoprecipitation demonstrated an interaction of PMCA4b and ZO-1. For the IP lysates of transfected HEK 293-PMCA4b cells, HEK 293 cells and ECV cells were precipitated with monoclonal antibody specific for PMCA4b and afterwards IB was performed with antibodies against ZO-1. The negative control was ECV cell lysate incubated with an irrelevant antibody (α-NFATc2) and the positive control was an input of the same cell lysate.

statistically different current densities (Figure 7(d)). However, the presence of nNOS led to a change in the voltage dependence of $Ca_v1.2$ Ba^{2+} currents (Figure 7(e)). To analyze the voltage dependence, normalized currents were plotted against their corresponding voltages of electrical stimulation, and the curve was fitted by the Boltzmann function to calculate basic parameters of voltage dependence, such as potential of half-maximal activation ($V_{1/2}$), and the steepness of the curve (k_{act}) (Figures 7(f)–7(i)). nNOS induced a shift of the voltage-dependent activation and the potential of maximal current amplitude towards more positive voltages. Statistical analysis of parameters of voltage dependence of wild-type $Ca_v1.2$ currents showed that the activation threshold of the currents was not changed (Figure 7(f)) but the potential of half-maximal activation $V_{1/2}$ was shifted from −3 to +1.5 mV (Figure 7(g)), which was due to a shift of the slope of the Boltzmann fitted curve (Figure 7(h)) and not due to a shift of the activation threshold. This shift in the voltage dependence resulted in a different potential of maximal current amplitude (Figure 7(i)).

4. Discussion

The voltage-gated L-type calcium channel, $Ca_v1.2$, and the plasma membrane calcium ATPase, PMCA4b, play major roles in excitable and nonexcitable cells. $Ca_v1.2$ regulates the calcium entry into cells upon depolarization, while PMCA4b controls cellular calcium homeostasis by calcium extrusion. Both are important functional proteins in the heart and brain, but the specific tasks and the precise mechanisms are still investigated. The present studies were initiated to understand the regulatory consequence and the physiological background of the interactions from the C-terminal ligands $Ca_v1.2$ and PMCA4b with PDZ domain containing proteins. Using three independent assays (PDZ Domain Array, GST pull-down, and immunoprecipitation) and colocalization studies, we could show the interaction of a multiplicity of PDZ domain containing proteins and their ligands, $Ca_v1.2$ and PMCA4b.

PDZ domain proteins regulate the traffic and targeting of proteins, to assembly of signaling complexes and networks designed for efficient and specific signal transduction [6]. Presently, some of the described interaction partners of PMCA4b belong to the family of MAGUKs [18, 23, 46] but, in addition, nNOS and NHERF2 have been identified as interacting partners of PMCA C-termini [28, 29]. The C-terminal end of the PMCA splice variant 4b (ETSV) differs from other b variants [16, 17, 28], suggesting that the C-termini determine the specificity of interactions with other proteins. We identified new PDZ protein interaction partners of PMCA4b, whereby ZO-1, MAGI-1-3, Mint-2, and MAST-205 are of primary importance. For $Ca_v1.2$, we detected the same combination of proteins, with the addition of CASK, NHERF1, NHERF2 and nNOS.

Zonula occludens proteins are regulators of tight junction (TJ) assembly, and recent investigations have shown that these proteins also promote adherens junction (AJ) assembly [47]. The protein binding between the PDZ domain 1 of ZO-1 and the C-terminus of PMCA4b is insofar likely because both proteins are located at the membrane (Figure 4(b), Supplemental Figure 2(C)). A similar interaction is observed between the C-terminus of $Ca_v1.2$ and the PDZ domains 1 and 2 of ZO-1 (Figure 3(d) and Supplemental Figure 2(B)). We suggest that this protein interaction is probably important for the regulation of calcium ions and cytoskeletal dynamics at cell junctions and the plasma membrane.

In our experiments we detected that the three MAGI proteins (MAGI-1 domain 3; MAGI-2 and MAGI-3 domain 6) bind to the C-terminus of PMCA4b and $Ca_v1.2$ (Figures 2(b)–2(c) and Figure 3(c)). MAGI-1 and MAGI-3 are widely expressed in tissues like brain, heart, lung, and colon, but tend to localize to tight junctions of epithelial cells [48, 49]. MAGI-2 is exclusively widespread in neuronal tissue [50]. The group of Hall [51, 52] reported that the β1 adrenergic receptor (β1AR) binds MAGI-2 and MAGI-3. MAGI-2 enhances the receptor's association with β-Catenin and its internalization, while MAGI-3 inhibits G_i-mediated ERK activation by β1AR. MAGI-2 and MAGI-3 also bind to the tumor suppressor gene product of PTEN (a tumor suppressor phosphatase). These MAGI proteins support PTEN suppression of Akt, which

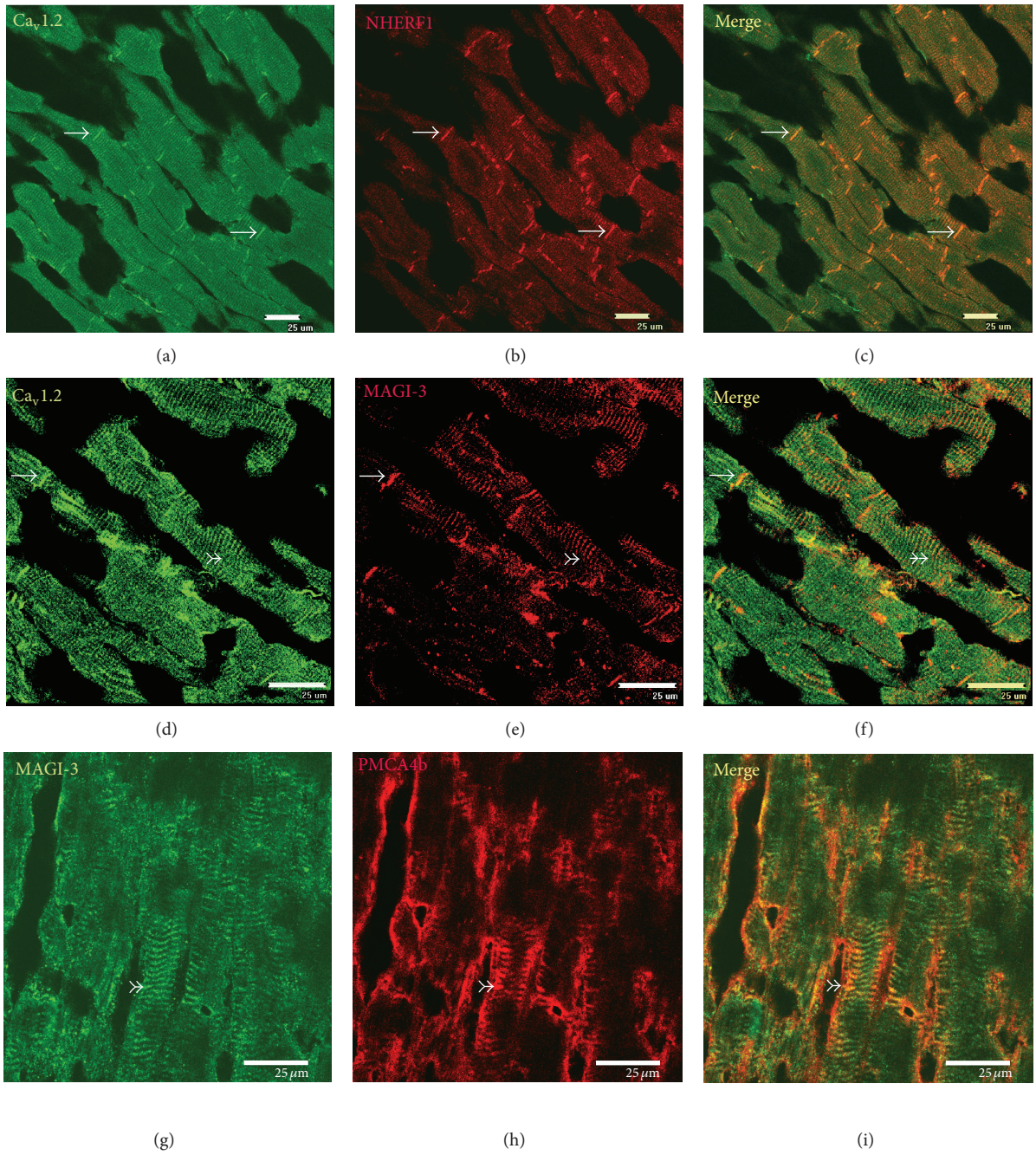

Figure 5: Colocalization of $Ca_v1.2$ with NHERF1 and MAGI-3, and PMCA4b with MAGI-3 in rat cardiomyocytes. Double immunofluorescent staining of $Ca_v1.2$ and NHERF1 ((a)–(c)), MAGI-3 and $Ca_v1.2$ ((d)–(f)), and PMCA4b and MAGI-3 ((g)–(i)) in rat cardiomyocytes. For heart sections the following antibodies were used: polyclonal rabbit anti-$Ca_v1.2$-ATTO 488 ((a), (d)), polyclonal rabbit anti-NHERF1 (b), polyclonal rabbit anti-MAGI-3 ((e), (g)), and monoclonal mouse anti-PMCA 5F10 (h) followed by Alexa Fluor 488 goat anti-mouse, or Alexa Fluor 594 goat anti-rabbit, where appropriate. (c), (f), and (i) are merged images. $Ca_v1.2$ and NHERF1 are coexpressed at the intercalated discs of cardiomyocytes (see arrow →), $Ca_v1.2$ and MAGI-3 at the intercalated discs and transverse tubules (T-tubuli) (see arrow ↠). PMCA4b and MAGI-3 are located at the T-tubules as well (see arrow ↠).

is involved in apoptosis suppression and growth induction [41, 53]. However, MAGI-3 is localized to diverse cellular compartments including the nucleus, cytoplasm, and junctional complexes at the cell surface [54], making it a central modulator of its function as scaffold protein. It is interesting that both of our investigated ligands, PMCA4b and $Ca_v1.2$, interact with all three MAGI proteins since the scaffolds are components of signaling complexes implicated in processes that require calcium. PMCA4b and $Ca_v1.2$ may play key roles in the arrangement of calcium-dependent AJs, and thus be

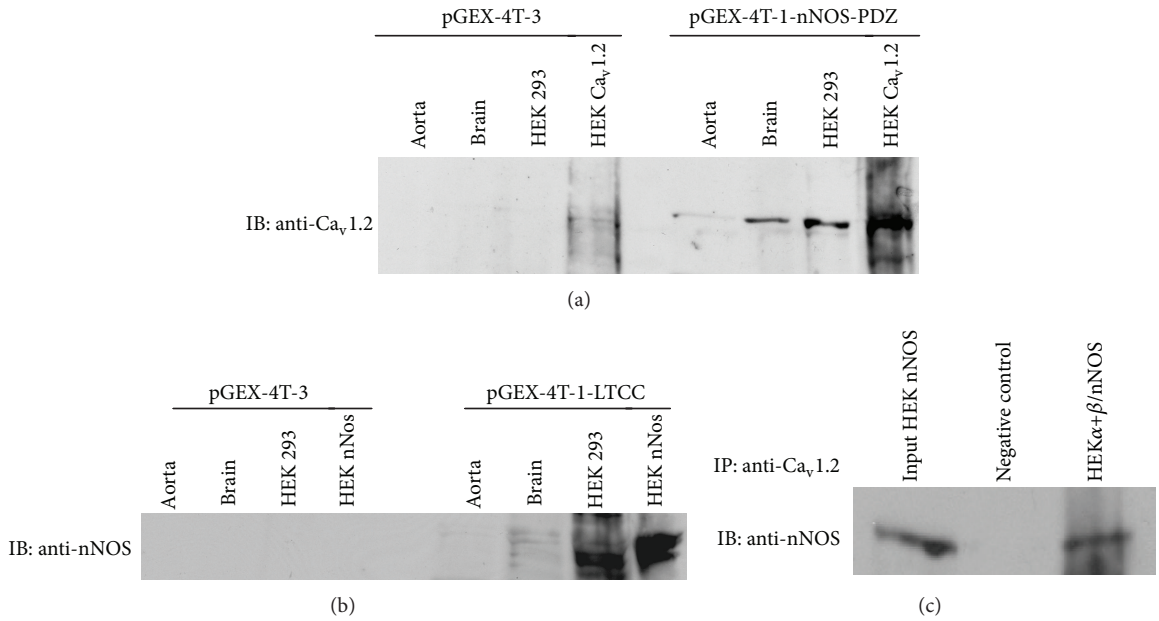

Figure 6: $Ca_v1.2\alpha$ C-terminal end interaction with PDZ domain of nNOS. (a) Lysates from mouse organs (aorta, brain) and lysates from untransfected HEK 293 cells and HEK 293 cells transfected with pcDNA3-$Ca_v1.2\alpha$ were incubated with Glutathione-Sepharose beads containing equal amounts of GST (pGEX-4T-3) and the nNOS PDZ domain fused to GST (pGEX-4T-1-nNOS-PDZ). For detection we used α-$Ca_v1.2$ (190–210 kDa). An interaction is observed between $Ca_v1.2\alpha$ and the GST fusion protein pGEX-4T-1-nNOS-PDZ, but not with GST. (b) Lysates were the same as described above. Here the HEK 293 cells were transfected with pcDNA3-nNOS. The negative control was GST (pGEX-4T-3). For detection we used α-nNOS (160 kDa). An interaction between nNOS to the fusion protein pGEX-4T-1-LTCC, where the final C-terminal 10 amino acids were fused to GST, was shown. (c) Coimmunoprecipitation demonstrated an interaction of $Ca_v1.2\alpha$ with nNOS. HEK 293 cells were transfected with pcDNA3-nNOS. 20 μg of the protein lysate was used directly as input for SDS-polyacrylamide gel electrophoresis. The negative controls were HEK 293 cells transfected with nNOS expression constructs immunoprecipitated with an irrelevant α-rabbit antibody (α-AT2), and the last lane contained HEK 293 cells (stably expressing the α and β subunits of $Ca_v1.2$) co-transfected with pcDNA3-nNOS, and immunoprecipitated with α-$Ca_v1.2$ antibody. For detection, we used the antibody α-nNOS.

Table 1: Summary of further investigated potential interaction partners.

Full name of protein	Accession	PDZ domain	Mean grey values	
			$Ca_v1.2$	PMCA4b
Calcium/calmodulin-dependent serine protein kinase (CASK)	O14936	CASK	11.0	4.4
Microtubule-associated testis specific serine/threonine protein kinase (MAST205)	Q6P0Q8	MAST205	77.7	53.5
Solute carrier family 9 (sodium/hydrogen exchanger) 3 regulatory factor 1 (NHERF1), domain 1	O14745	NHERF1-D1	84.8	0
Tight junction protein 1 (Zonula occludens) Z01, domain 1	Q07157	Z01-D1	130.7	40.6
Nitric oxide synthase 1 (neuronal) nNOS, domain 5	P29475	nNOS	36.2	0
Membrane-associated guanylate kinase-related 3 (MAGI-3), domain 6	Q5TCQ9	MAGI3-D6	72.7	203.3

involved in regulation of cell growth, cell morphology, and cell differentiation.

The Mint protein family (muc18-1-interacting protein) has three members, Mint-1, Mint-2, and Mint-3 [55, 56]. The Mint family plays a role in the arrangement of multiprotein complexes, and their ability to control the signaling and trafficking of membrane proteins [57]. Mints bind to Munc-18, a protein necessary for synaptic vesicle exocytosis, and to CASK, which is involved in targeting and localization of synaptic membrane proteins [55, 58–63]. The presence of PDZ domains in Mints indicates a potential involvement of these proteins in connecting synaptic vesicles to the sites of synaptic intercellular junctions [24]. The multiprotein complex between our investigated ligands and Mint proteins could play a role in the exocytosis of synaptic vesicles, as the process requires a Ca^{2+} trigger and the resultant release of neurotransmitters is a Ca^{2+}-dependent reaction (Supplemental data).

MAST-205 (microtubule-associated serine/threonine kinase) is highly expressed in testis [44] and in kidney, adrenal glands, hindbrain, small intestine, and colon tissues [45]. This protein possesses a Ser/Thr kinase and one PDZ domain. Few protein interactions with MAST-205 have been identified. For example, the PDZ domain of MAST-205 additionally binds to PTEN, which regulates the cell growth and apoptosis [64]. The phosphorylation

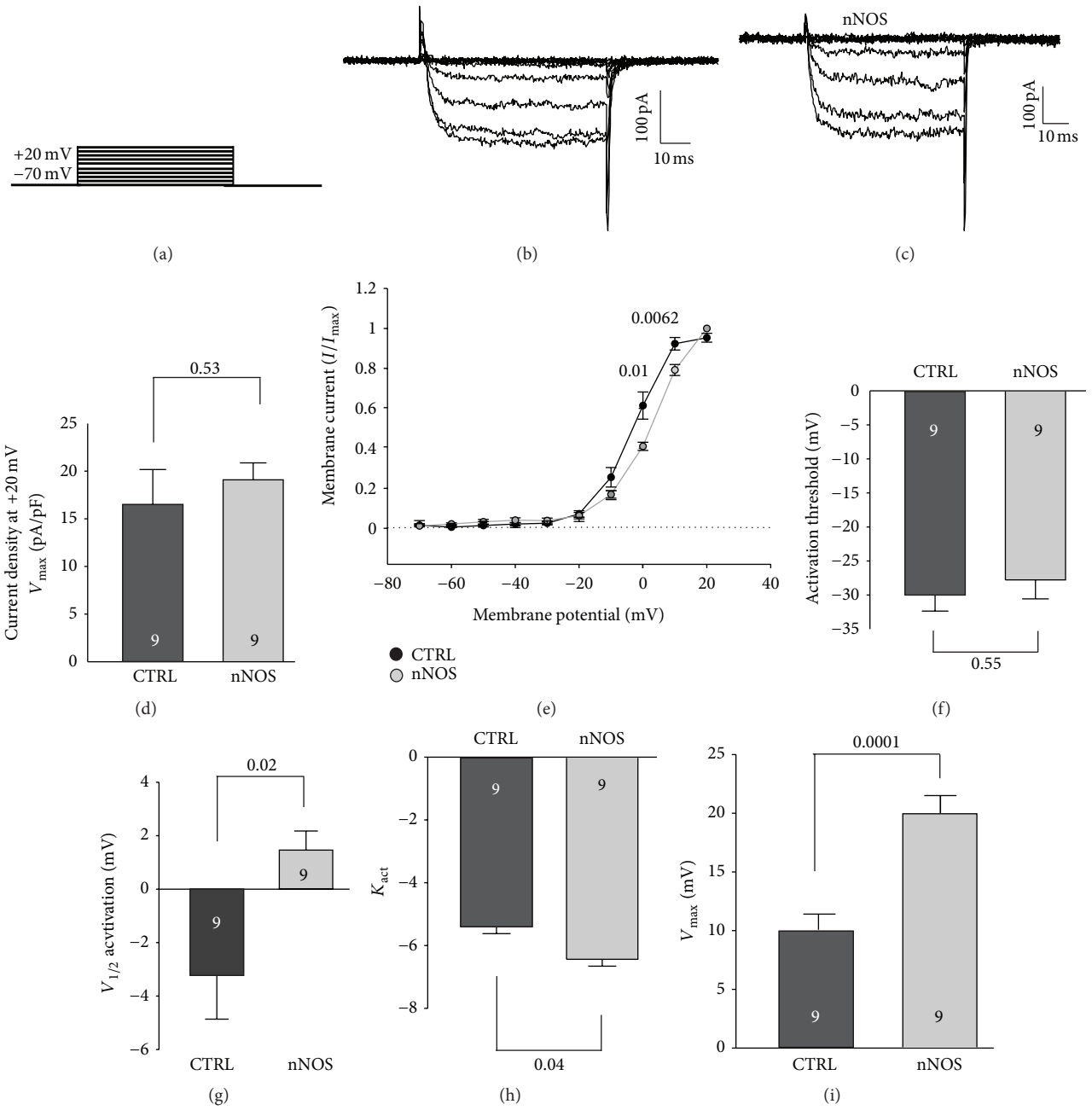

Figure 7: Electrophysiological properties of Ba^{2+} currents from $Ca_v1.2$ subunits. (a) Pattern of electrical stimulation. The membrane potential was clamped at a holding potential of −70 mV. From the holding potential the cells were depolarized by nine voltage steps with +10 mV incremental amplitudes and 50 ms duration. (b) Ba^{2+} currents induced by the electrical stimulation shown in (a) in a cell expressing wild-type $Ca_v1.2$ channels. (c) $Ca_v1.2$ channel Ba^{2+} currents induced by the electrical stimulation shown in (a) in a cell expressing nNOS. (d) Maximal current density of control $Ca_v1.2$ currents, $Ca_v1.2$ subunits in the presence of nNOS. (e) Voltage dependence of Ba^{2+} currents: currents were normalized to the maximal current amplitude and plotted against the potentials of the electrical stimulation; the curve was fitted using the Boltzmann equation. (f) Activation threshold of Ba^{2+} currents from $Ca_v1.2$ subunits and $Ca_v1.2$ subunits in the presence of nNOS; the numbers indicate the level of significance. (g) Voltage of half-maximal activation Ba^{2+} currents from $Ca_v1.2$ subunits and $Ca_v1.2$ subunits in the presence of nNOS; the potentials of half-maximal activation were significantly shifted towards positive potentials in the presence of nNOS. (h) Slope of Boltzmann curve (k_{act}) of Ba^{2+} currents from $Ca_v1.2$ subunits and $Ca_v1.2$ subunits in the presence of nNOS; the k_{act} values were significantly larger in the presence of nNOS. (i) Comparison of the voltages of maximal current amplitudes (V_{max}); in the presence of nNOS V_{max} was shifted towards more positive voltages of currents from $Ca_v1.2$ subunits.

of PTEN by the kinase domain of MAST-205 suggests that PTEN could be a physiological substrate. The group of Yun demonstrated that MAST-205 modulates the transport activity of Na^+/H^+exchanger (NHE3) in the renal proximal tubule, and this regulation was dependent on the presence of the kinase motif in MAST-205 [45]. Our studies suggest that the C-terminal tail of PMCA4b and $Ca_v1.2$ may act as component for specific and efficient PDZ domain recognition, which could be important in the control of PMCA4b and $Ca_v1.2$ protein phosphorylation, stability, and function (Figure 3(e), Supplemental Figures 2(B)-2(C)).

We identified the PDZ domain containing protein CASK as a functional interaction partner of $Ca_v1.2$ (Supplemental Figures 1(B) and 3(A)). The MAGUK protein CASK consists of a Ca^{2+}-calmodulin kinase, a PDZ domain, an SH3 domain, and a guanylate kinase domain. It is mainly expressed at the neuronal presynaptic membrane, interacting with neuroligin-associated neurexin [65–67], and additionally expressed in epithelial cells [37]. Mutation or deletion of CASK results in unusual synaptic function and perinatal death in mice [65], verifying its importance for brain development and function. CASK controls synapse formation and synaptic strength, and mutation or deletion in the gene leads to mental retardation [68]. All these studies indicate that $Ca_v1.2$ and PMCA4b in conjunction with CASK may play vital roles in the targeting of protein complexes in brain and epithelial cells, and in the modulation of synaptic transmission.

Other interesting interaction partners are the sodium-hydrogen exchanger regulatory factors, NHERF1 (also called EBP50) and NHERF2 (called E3KARP). In coexistence, they possess overlapping function as regulators of transmembrane receptors, transporters, and other proteins localized at or near the plasma membrane. The ERM (Ezrin, Radixin, Moesin, and Merlin) family of membrane cytoskeletal adapters is a crucial cellular target of NHERF [69, 70]. To regulate NHE3 signaling with cAMP, NHERF1 (or NHERF2), Ezrin, and protein kinase A form a multiprotein signal complex connecting NHE3 to the actin cytoskeleton. This complex is proposed to facilitate the phosphorylation and downregulation of NHE3 [70–72], playing a crucial role in the proximal tubule, because H^+ is secreted into the lumen by NHE3, essentially maintaining the acid base balance of the kidney. Another important aspect is the relationship between NHERF and CFTR (cystic fibrosis transmembrane regulator). The interaction between CFTR and NHERF may explain CFTRs ability to regulate other transport proteins, including the epithelial sodium channel, the renal outer medullary potassium channel, and NHE3 [73, 74]. Demarco et al. 2002 [28] suggested that the PDZ domains of NHERF1/2 bind the D-(S/T)-X-L motif (X represents any amino acid) at C-termini. Therefore, with the exception of PMCA4b, which has an ETSV motif, PMCAs 1b–3b (motif ETSL) interact with NHERF1/2. We confirmed these results with the PDZ Domain Array (Supplemental Figure 2(C)). Additionally, we identified a new interaction between NHERF1/2 with $Ca_v1.2$ (motif VSNL) in Supplemental Figure 2(B). Our findings and previous studies from other groups emphasize the importance of a terminal leucine residue for high affinity peptide interaction with NHERF [28, 75, 76]. The complex of $Ca_v1.2$ and NHERF1/2 may provide an indirect link between the Ca^{2+} channel and the actin cytoskeletal network, especially to stabilize the channel along the membrane and to allow its regulation by coassembled cAMP-dependent protein kinases. The PDZ domain 1 of NHERF1 is associated with SOCs (store operated calcium channel), Trp4, Trp5, and the phospholipases Cβ1 and Cβ2 [77], suggesting that NHERF can link the functions of SOCs to PLCβ to organize calcium and phosphoinositide metabolism, and control cell metabolism and growth. Our new results suggest an involvement of NHERF1/2 in the regulation of Ca^{2+} transport as well.

The colocalization of $Ca_v1.2$ and NHERF1 at intercalated discs and of $Ca_v1.2$ and MAGI-3 at the intercalated discs and the transverse tubules is noteworthy (Figures 5(a)–5(f)). The same applies for PMCA4b and MAGI-3 at transverse tubules (Figures 5(g)–5(i)). The intercalated discs of cardiomyocytes are crucial for pulse transmission and cell structure stabilization. The transverse tubules are invaginations of the plasma membrane of muscle cells that facilitate faster transfer of a depolarisation from the plasma membrane to the core of the cell. PMCA4b and $Ca_v1.2$ are both expressed at the caveolae of the plasma membrane, as mentioned above.

nNOS plays a crucial role in cardiomyocytes [78], regulating excitation-contraction coupling [79, 80], β-adrenergic inotropic response [79], and the development of heart failure [81, 82]. nNOS has been localized to the sarcolemma and the sarcoplasmic reticulum (SR) [29, 83, 84]. We have established that the C-terminus of $Ca_v1.2$ interacts with the PDZ domain of nNOS by means of a PDZ Domain Array, IP, and GST pull-down (Figures 6(a)–6(c), Supplemental Figure 2(B)). Burkard et al. presented data from nNOS overexpressing mice that showed the negative inotropic effect of myocardial nNOS, which can reduce Ca^{2+} currents of $Ca_v1.2$ in their model system [85]. Furthermore, Sears et al. postulate that nNOS regulates Ca^{2+} influx by means of negative feedback, because increases in $[Ca^{2+}]_i$ excite nNOS synthesis of NO, which, on the other hand, inhibits Ca^{2+} influx [80]. We now confirmed these studies by measurements of Ca^{2+} currents in stable HEK 293 cells, transfected with nNOS.

The cells, which express $Ca_v1.2$ subunits showed Ba^{2+} currents with properties of L-type Ca^{2+} channels. The activation threshold and voltage of half-maximal activation are corresponding to that, which is commonly known for the cardiac subtype of L-type channels that corresponds with the $Ca_v1.2$ subunit. The Ba^{2+} currents from the cells, which stably express $Ca_v1.2$ subunits showed no inactivation. This can be due to the fact that Ba^{2+} was used instead of Ca^{2+}, which normally leads to loss of inactivation. Furthermore, the presence of inactivation is dependent on the coexpressed β-subunit. Upon nNOS expression only the voltage-dependent activation was changed. In the presence of nNOS the voltage-dependent activation was shifted towards more positive potentials and a change of the steepness of the curve of voltage-dependent activation resulted in shift in the voltage of maximal current amplitude while the activation threshold was unchanged. Thus, in the presence of nNOS, $Ca_v1.2$

subunits can be activated by the same depolarizing voltage difference but due to the shift of the half-maximal activation the currents amplitudes were smaller. With this effect, the Ca^{2+} channel current is reduced, resulting in a smaller voltage-dependent Ca^{2+} increase. In cells which express $Ca_v1.2$ subunits Ca^{2+}-dependent function would be reduced. For example, smooth muscle cells expressing active nNOS would display smaller depolarization-induced contractions and would support NOS-dependent relaxation.

In summary, we showed that $Ca_v1.2$ interacts physically with nNOS-, MAST-205-, MAGI-3-, NHERF1-, and ZO-1-PDZ domains; and PMCA4b with ZO-1-, MAST-205-, and MAGI-3-PDZ domains, all demonstrated via different assays (PDZ array, GST pull-down, and IP). The partial colocalization of $Ca_v1.2$ and MAGI-3, $Ca_v1.2$ and NHERF1, and PMCA4b and MAGI-3 in rat cardiomyocytes indicates that an interaction of these proteins is highly possible. From our results, we conclude that $Ca_v1.2$ and PMCA4b bind promiscuously to a variety of PDZ domains. The physiological consequence of some of these interactions remains to be investigated.

Abbreviations

PSD-95:	Postsynaptic density protein 95
SAP 90:	Synapse-associated protein 90
PSD-93 (Chapsyn-110):	Channel-associated protein of synapse-110
SH3 domain:	Src homology 3domain
RIL:	Reversion-induced LIM protein
SCRIB1:	Scribble domain 1
TIP1:	Tax interaction protein 1
OMP25:	Mitochondrial outer membrane protein 25
MUPP:	Multiple PDZ domain protein
hCLIM1:	Human 36 kDa carboxyl terminal LIM domain protein
HtrA2:	High temperature requirement protein A2
hPTP1E-D1:	Protein tyrosine phosphatase 1E-domain 1.

Acknowledgments

The authors thank Dr. Andrea Welling (Institute of Pharmacology and Toxicology, TU Munich) for providing the stably transfected HEK 293 cells (α_{1b} and β2a subunit of $Ca_v1.2$). The authors greatly appreciate the gift of the plasmid constructs, pGEX-4T-1-nNOS-PDZ, and pcDNA3-nNOS from Dr. Bredt (University of California, San Francisco, USA) and Rafael Pulido (Centro de Investigacion Principe Felipe, Valencia, Spain) for pRK5-kinase-MAST-205 and pRK5-kinase-PDZ-MAST-205. The work was supported by the IZKF Wuerzburg, TP E-33 to KS.

References

[1] K. O. Cho, C. A. Hunt, and M. B. Kennedy, "The rat brain postsynaptic density fraction contains a homolog of the Drosophila discs-large tumor suppressor protein," *Neuron*, vol. 9, no. 5, pp. 929–942, 1992.

[2] A. S. Fanning and J. M. Anderson, "Protein modules as organizers of membrane structure," *Current Opinion in Cell Biology*, vol. 11, no. 4, pp. 432–439, 1999.

[3] M. B. Kennedy, "Origin of PDZ (DHR, GLGF) domains," *Trends in Biochemical Sciences*, vol. 20, no. 9, p. 350, 1995.

[4] E. Kim, M. Niethammer, A. Rothschild, Y. N. Jan, and M. Sheng, "Clustering of Shaker-type K^+ channels by interaction with a family of membrane-associated guanylate kinases," *Nature*, vol. 378, no. 6552, pp. 85–88, 1995.

[5] H. C. Kornau, P. H. Seeburg, and M. B. Kennedy, "Interaction of ion channels and receptors with PDZ domain proteins," *Current Opinion in Neurobiology*, vol. 7, no. 3, pp. 368–373, 1997.

[6] C. Nourry, S. G. Grant, and J. P. Borg, "PDZ domain proteins: plug and play!," *Science's STKE*, vol. 2003, no. 179, p. RE7, 2003.

[7] D. F. Woods and P. J. Bryant, "ZO-1, DlgA and PSD-95/SAP90: homologous proteins in tight, septate and synaptic cell junctions," *Mechanisms of Development*, vol. 44, no. 2-3, pp. 85–89, 1993.

[8] J. N. Muth, H. Yamaguchi, G. Mikala et al., "Cardiac-specific overexpression of the α1 subunit of the L-type voltage-dependent Ca^{2+} channel in transgenic mice. Loss of isoproterenol-induced contraction," *Journal of Biological Chemistry*, vol. 274, no. 31, pp. 21503–21506, 1999.

[9] L.-S. Song, A. Guia, J. N. Muth et al., "Ca^{2+} signaling in cardiac myocytes overexpressing the α_1 subunit of L-type Ca^{2+} channel," *Circulation Research*, vol. 90, no. 2, pp. 174–181, 2002.

[10] C. Seisenberger, V. Specht, A. Welling et al., "Functional embryonic cardiomyocytes after disruption of the L-type α1C (Ca_v 1.2) calcium channel gene in the mouse," *Journal of Biological Chemistry*, vol. 275, no. 50, pp. 39193–39199, 2000.

[11] M. Xu, A. Welling, S. Paparisto, F. Hofmann, and N. Klugbauer, "Enhanced expression of L-type $Ca_v1.3$ calcium channels in murine embryonic hearts from $Ca_v1.2$-deficient Mice," *Journal of Biological Chemistry*, vol. 278, no. 42, pp. 40837–40841, 2003.

[12] I. Splawski, K. W. Timothy, N. Decher et al., "Severe arrhythmia disorder caused by cardiac L-type calcium channel mutations," *Proceedings of the National Academy of Sciences of the United States of America*, vol. 102, no. 23, pp. 8089–8096, 2005.

[13] I. Splawski, K. W. Timothy, L. M. Sharpe et al., "$Ca_v1.2$ calcium channel dysfunction causes a multisystem disorder including arrhythmia and autism," *Cell*, vol. 119, no. 1, pp. 19–31, 2004.

[14] M. L. Garcia and E. E. Strehler, "Plasma membrane calcium ATPases as critical regulators of calcium homeostasis during neuronal cell function," *Frontiers in Bioscience*, vol. 4, pp. D869–D882, 1999.

[15] G. R. Monteith and B. D. Roufogalis, "The plasma membrane calcium pump—a physiological perspective on its regulation," *Cell Calcium*, vol. 18, no. 6, pp. 459–470, 1995.

[16] J. T. Penniston and A. Enyedi, "Modulation of the plasma membrane Ca^{2+} pump," *Journal of Membrane Biology*, vol. 165, no. 2, pp. 101–109, 1998.

[17] E. E. Strehler and D. A. Zacharias, "Role of alternative splicing in generating isoform diversity among plasma membrane calcium pumps," *Physiological Reviews*, vol. 81, no. 1, pp. 21–50, 2001.

[18] S. J. DeMarco and E. E. Strehler, "Plasma membrane Ca^{2+}-atpase isoforms 2b and 4b interact promiscuously and selectively with members of the membrane-associated guanylate kinase family of PDZ (PSD95/Dlg/ZO-1) domain-containing proteins," *Journal of Biological Chemistry*, vol. 276, no. 24, pp. 21594–21600, 2001.

[19] T. Fujimoto, "Calcium pump of the plasma membrane is localized in caveolae," *Journal of Cell Biology*, vol. 120, no. 5, pp. 1147–1158, 1993.

[20] A. Hammes, S. Oberdorf-Maass, T. Rother et al., "Overexpression of the sarcolemmal calcium pump in the myocardium of transgenic rats," *Circulation Research*, vol. 83, no. 9, pp. 877–888, 1998.

[21] B. Razani, S. E. Woodman, and M. P. Lisanti, "Caveolae: from cell biology to animal physiology," *Pharmacological Reviews*, vol. 54, no. 3, pp. 431–467, 2002.

[22] P. W. Shaul and R. G. W. Anderson, "Role of plasmalemmal caveolae in signal transduction," *American Journal of Physiology*, vol. 275, no. 5, pp. L843–L851, 1998.

[23] K. Schuh, S. Uldrijan, S. Gambaryan, N. Roethlein, and L. Neyses, "Interaction of the plasma membrane Ca^{2+} pump 4b/CI with the Ca^{2+}/calmodulin-dependent membrane-associated kinase CASK," *Journal of Biological Chemistry*, vol. 278, no. 11, pp. 9778–9783, 2003.

[24] S. N. Gomperts, "Clustering membrane proteins: it's all coming together with the PSD-95/SAP90 protein family," *Cell*, vol. 84, no. 5, pp. 659–662, 1996.

[25] L. A. Lasky, N. J. Skelton, and S. S. Siduh, "PDZ domains: intracellular mediators of carboxy-terminal protein recognition and scaffolding," in *Modular Protein Domains*, G. Cesareni, M. Gimona, M. Sudol, and M. Yaffe, Eds., pp. 257–273, WILEY-VCH Verlag GmbH & Co, Weinheim, Germany, 2005.

[26] J. M. Montgomery, P. L. Zamorano, and C. C. Garner, "MAGUKs in synapse assembly and function: an emerging view," *Cellular and Molecular Life Sciences*, vol. 61, no. 7-8, pp. 911–929, 2004.

[27] G. M. Goellner, S. J. DeMarco, and E. E. Strehler, "Characterization of PISP, a novel single-PDZ protein that binds to all plasma membrane Ca^{2+}-ATPase b-splice variants," *Annals of the New York Academy of Sciences*, vol. 986, pp. 461–471, 2003.

[28] S. J. Demarco, M. C. Chicka, and E. E. Strehler, "Plasma membrane Ca^{2+} ATPase isoform 2b interacts preferentially with Na+/H+ exchanger regulatory factor 2 in apical plasma membranes," *Journal of Biological Chemistry*, vol. 277, no. 12, pp. 10506–10511, 2002.

[29] K. Schuh, S. Uldrijan, M. Telkamp, N. Röthlein, and L. Neyses, "The plasmamembrane calmodulin-dependent calcium pump: a major regulator of nitric oxide synthase I," *Journal of Cell Biology*, vol. 155, no. 2, pp. 201–205, 2001.

[30] A. L. Armesilla, J. C. Williams, M. H. Buch et al., "Novel functional interaction between the plasma membrane Ca^{2+} pump 4b and the proapoptotic tumor suppressor Ras-associated factor 1 (RASSF1)," *Journal of Biological Chemistry*, vol. 279, no. 30, pp. 31318–31328, 2004.

[31] M. H. Bucht, A. Pickard, A. Rodriguez et al., "The sarcolemmal calcium pump inhibits the calcineurin/nuclear factor of activated T-cell pathway via interaction with the calcineurin A catalytic subunit," *Journal of Biological Chemistry*, vol. 280, no. 33, pp. 29479–29487, 2005.

[32] J. P. Williams, T. Stewart, B. Li, R. Mulloy, D. Dimova, and M. Classon, "The retinoblastoma protein is required for Ras-induced oncogenic transformation," *Molecular and Cellular Biology*, vol. 26, no. 4, pp. 1170–1182, 2006.

[33] U. K. Laemmli, "Cleavage of structural proteins during the assembly of the head of bacteriophage T4," *Nature*, vol. 227, no. 5259, pp. 680–685, 1970.

[34] C. Seisenberger, A. Welling, A. Schuster, and F. Hofmann, "Two stable cell lines for screening of calcium channel blockers," *Naunyn-Schmiedeberg's Archives of Pharmacology*, vol. 352, no. 6, pp. 662–669, 1995.

[35] X. Zong, J. Schreieck, G. Mehrke et al., "On the regulation of the expressed L-type calcium channel by cAMP-dependent phosphorylation," *Pflugers Archiv*, vol. 430, no. 3, pp. 340–347, 1995.

[36] S. Hjertén, "A new method for preparation of agarose for gel electrophoresis," *Biochimica et Biophysica Acta*, vol. 62, no. 3, pp. 445–449, 1962.

[37] Y. Hata, S. Butz, and T. C. Südhof, "CASK: a novel dlg/PSD95 homolog with an N-terminal calmodulin-dependent protein kinase domain identified by interaction with neurexins," *Journal of Neuroscience*, vol. 16, no. 8, pp. 2488–2494, 1996.

[38] E. J. Weinman, D. Steplock, K. Tate, R. A. Hall, R. F. Spurney, and S. Shenolikar, "Structure-function of recombinant Na/H exchanger regulatory factor (NHE- RF)," *Journal of Clinical Investigation*, vol. 101, no. 10, pp. 2199–2206, 1998.

[39] H. Nakanishi, H. Obaishi, A. Satoh et al., "Neurabin: a novel neural tissue-specific actin filament-binding protein involved in neurite formation," *Journal of Cell Biology*, vol. 139, no. 4, pp. 951–961, 1997.

[40] J. D. Wood, J. Yuan, R. L. Margolis et al., "Atrophin-1, the DRPLA gene product, interacts with two families of WW domain-containing proteins," *Molecular and Cellular Neurosciences*, vol. 11, no. 3, pp. 149–160, 1998.

[41] Y. Wu, D. Dowbenko, S. Spencer et al., "Interaction of the tumor suppressor PTEN/MMAC with a PDZ domain of MAGI3, a novel membrane-associated guanylate kinase," *Journal of Biological Chemistry*, vol. 275, no. 28, pp. 21477–21485, 2000.

[42] J. M. Anerson, B. R. Stevenson, L. A. Jesaitis, D. A. Goodenough, and M. S. Mooseker, "Characterization of ZO-1, a protein component of the tight junction from mouse liver and Madin-Darby canine kidney cells," *Journal of Cell Biology*, vol. 106, no. 4, pp. 1141–1149, 1988.

[43] B. R. Stevenson, J. D. Siliciano, and M. S. Mooseker, "Identification of ZO-1: a high molecular weight polypeptide associated with the tight junction (Zonula Occludens) in a variety of epithelia," *Journal of Cell Biology*, vol. 103, no. 3, pp. 755–766, 1986.

[44] P. D. Walden and N. J. Cowan, "A novel 205-kilodalton testis-specific serine/threonine protein kinase associated with microtubules of the spermatid manchette," *Molecular and Cellular Biology*, vol. 13, no. 12, pp. 7625–7635, 1993.

[45] D. Wang, J. L. Hye, D. S. Cooper et al., "Coexpression of MAST205 inhibits the activity of Na^+/H^+ exchanger NHE3," *American Journal of Physiology*, vol. 290, no. 2, pp. F428–F437, 2006.

[46] E. Kim, S. J. DeMarco, S. M. Marfatia, A. H. Chishti, M. Sheng, and E. E. Strehler, "Plasma membrane Ca^{2+} ATPase isoform 4B binds to membrane-associated guanylate kinase (MAGUK) proteins via their PDZ (PSD-95/Dlg/ZO-1) domains," *Journal of Biological Chemistry*, vol. 273, no. 3, pp. 1591–1595, 1998.

[47] A. S. Fanning and J. M. Anderson, "Zonula occludens-1 and -2 are cytosolic scaffolds that regulate the assembly of cellular junctions," *Annals of the New York Academy of Sciences*, vol. 1165, pp. 113–120, 2009.

[48] J. L. Franklin, K. Yoshiura, P. J. Dempsey et al., "Identification of MAGI-3 as a transforming growth factor-α tail binding protein," *Experimental Cell Research*, vol. 303, no. 2, pp. 457–470, 2005.

[49] R. P. Laura, S. Ross, H. Koeppen, and L. A. Lasky, "MAGI-1: a widely expressed, alternatively spliced tight junction protein," *Experimental Cell Research*, vol. 275, no. 2, pp. 155–170, 2002.

[50] J. Iida, S. Hirabayashi, Y. Sato, and Y. Hata, "Synaptic scaffolding molecule is involved in the synaptic clustering of neuroligin," *Molecular and Cellular Neuroscience*, vol. 27, no. 4, pp. 497–508, 2004.

[51] J. He, M. Bellini, H. Inuzuka et al., "Proteomic analysis of β1-adrenergic receptor interactions with PDZ scaffold proteins," *Journal of Biological Chemistry*, vol. 281, no. 5, pp. 2820–2827, 2006.

[52] J. Xu, M. Paquet, A. G. Lau, J. D. Wood, C. A. Ross, and R. A. Hall, "beta 1-adrenergic receptor association with the synaptic scaffolding protein membrane-associated guanylate kinase inverted-2 (MAGI-2). Differential regulation of receptor internalization by MAGI-2 and PSD-95," *Journal of Biological Chemistry*, vol. 276, no. 44, pp. 41310–41317, 2001.

[53] X. Wu, K. Hepner, S. Castelino-Prabhu et al., "Evidence for regulation of the PTEN tumor suppressor by a membrane-localized multi-PDZ domain containing scaffold protein MAGI-2," *Proceedings of the National Academy of Sciences of the United States of America*, vol. 97, no. 8, pp. 4233–4238, 2000.

[54] K. Adamsky, K. Arnold, H. Sabanay, and E. Peles, "Junctional protein MAGI-3 interacts with receptor tyrosine phosphatase β (RPTPβ) and tyrosine-phosphorylated proteins," *Journal of Cell Science*, vol. 116, no. 7, pp. 1279–1289, 2003.

[55] M. Okamoto and T. C. Südhof, "Mints, munc18-interacting proteins in synaptic vesicle exocytosis," *Journal of Biological Chemistry*, vol. 272, no. 50, pp. 31459–31464, 1997.

[56] M. Okamoto and T. C. Südhof, "Mint 3: a ubiquitous mint isoform that does not bind to munc18-1 or -2," *European Journal of Cell Biology*, vol. 77, no. 3, pp. 161–165, 1998.

[57] B. Rogelj, J. C. Mitchell, C. C. J. Miller, and D. M. McLoughlin, "The X11/Mint family of adaptor proteins," *Brain Research Reviews*, vol. 52, no. 2, pp. 305–315, 2006.

[58] S. Ferro-Novick and R. Jahn, "Vesicle fusion from yeast to man," *Nature*, vol. 370, no. 6486, pp. 191–193, 1994.

[59] K. Hill, Y. Li, M. Bennett et al., "Munc18 interacting proteins: ADP-ribosylation factor-dependent coat proteins that regulate the traffic of β-Alzheimer's precursor protein," *Journal of Biological Chemistry*, vol. 278, no. 38, pp. 36032–36040, 2003.

[60] T. F. J. Martin, "Stages of regulated exocytosis," *Trends in Cell Biology*, vol. 7, no. 7, pp. 271–276, 1997.

[61] T. C. Sudhof, "The synaptic vesicle cycle: a cascade of protein-protein interactions," *Nature*, vol. 375, no. 6533, pp. 645–653, 1995.

[62] R. S. Zucker, "Exocytosis: a molecular and physiological perspective," *Neuron*, vol. 17, no. 6, pp. 1049–1055, 1996.

[63] S. Butz, M. Okamoto, and T. C. Südhof, "A tripartite protein complex with the potential to couple synaptic vesicle exocytosis to cell adhesion in brain," *Cell*, vol. 94, no. 6, pp. 773–782, 1998.

[64] M. Valiente, A. Andrés-Pons, B. Gomar et al., "Binding of PTEN to specific PDZ domains contributes to PTEN protein stability and phosphorylation by microtubule-associated serine/threonine kinases," *Journal of Biological Chemistry*, vol. 280, no. 32, pp. 28936–28943, 2005.

[65] D. Atasoy, S. Schoch, A. Ho et al., "Deletion of CASK in mice is lethal and impairs synaptic function," *Proceedings of the National Academy of Sciences of the United States of America*, vol. 104, no. 7, pp. 2525–2530, 2007.

[66] M. Irie, Y. Hata, M. Takeuchi et al., "Binding of neuroligins to PSD-95," *Science*, vol. 277, no. 5331, pp. 1511–1515, 1997.

[67] A. T. Suckow, D. Comoletti, M. A. Waldrop et al., "Expression of neurexin, neuroligin, and their cytoplasmic binding partners in the pancreatic β-cells and the involvement of neuroligin in insulin secretion," *Endocrinology*, vol. 149, no. 12, pp. 6006–6017, 2008.

[68] Y. P. Hsueh, "Calcium/calmodulin-dependent serine protein kinase and mental retardation," *Annals of Neurology*, vol. 66, no. 4, pp. 438–443, 2009.

[69] A. Murthy, C. Gonzalez-Agosti, E. Cordero et al., "NHE-RF, a regulatory cofactor for Na^+-H^+ exchange, is a common interactor for merlin and ERM (MERM) proteins," *Journal of Biological Chemistry*, vol. 273, no. 3, pp. 1273–1276, 1998.

[70] D. Reczek, M. Berryman, and A. Bretscher, "Identification of EPB50: a PDZ-containing phosphoprotein that associates with members of the ezrin-radixin-moesin family," *Journal of Cell Biology*, vol. 139, no. 1, pp. 169–179, 1997.

[71] E. J. Weinman, "New functions for the NHERF family of proteins," *Journal of Clinical Investigation*, vol. 108, no. 2, pp. 185–186, 2001.

[72] E. J. Weinman, C. Minkoff, and S. Shenolikar, "Signal complex regulation of renal transport proteins: NHERF and regulation of NHE3 by PKA," *American Journal of Physiology*, vol. 279, no. 3, pp. F393–F399, 2000.

[73] B. D. Moyer, J. Demon, K. H. Karlson et al., "A PDZ-interacting domain in CFTR is an apical membrane polarization signal," *Journal of Clinical Investigation*, vol. 104, no. 10, pp. 1353–1361, 1999.

[74] V. Raghuram, D. O. D. Mak, and J. K. Foskett, "Regulation of cystic fibrosis transmembrane conductance regulator single-channel gating by bivalent PDZ-domain-mediated interaction," *Proceedings of the National Academy of Sciences of the United States of America*, vol. 98, no. 3, pp. 1300–1305, 2001.

[75] R. A. Hall, L. S. Ostedgaard, R. T. Premont et al., "A C-terminal motif found in the β2-adrenergic receptor, P2Y1 receptor and cystic fibrosis transmembrane conductance regulator determines binding to the Na+/H+ exchanger regulatory factor family of PDZ proteins," *Proceedings of the National Academy of Sciences of the United States of America*, vol. 95, no. 15, pp. 8496–8501, 1998.

[76] B. D. Moyer, M. Duhaime, C. Shaw et al., "The PDZ-interacting domain of cystic fibrosis transmembrane conductance regulator is required for functional expression in the apical plasma membrane," *Journal of Biological Chemistry*, vol. 275, no. 35, pp. 27069–27074, 2000.

[77] Y. Tang, J. Tang, Z. Chen et al., "Association of mammalian Trp4 and phospholipase C isozymes with a PDZ domain-containing protein, NHERF," *Journal of Biological Chemistry*, vol. 275, no. 48, pp. 37559–37564, 2000.

[78] M. V. Brahmajothi and D. L. Campbell, "Heterogeneous basal expression of nitric oxide synthase and superoxide dismutase isoforms in mammalian heart: implications for mechanisms governing indirect and direct nitric oxide-related effects," *Circulation Research*, vol. 85, no. 7, pp. 575–587, 1999.

[79] L. A. Barouch, R. W. Harrison, M. W. Skaf et al., "Nitric oxide regulates the heart by spatial confinement of nitric oxide synthase isoforms," *Nature*, vol. 416, no. 6878, pp. 337–340, 2002.

[80] C. E. Sears, S. M. Bryant, E. A. Ashley et al., "Cardiac neuronal nitric oxide synthase isoform regulates myocardial contraction and calcium handling," *Circulation Research*, vol. 92, no. 5, pp. e52–e59, 2003.

[81] J. K. Bendall, T. Damy, P. Ratajczak et al., "Role of myocardial neuronal nitric oxide synthase-derived nitric oxide in β-adrenergic hyporesponsiveness after myocardial infarction-induced heart failure in rat," *Circulation*, vol. 110, no. 16, pp. 2368–2375, 2004.

[82] T. Damy, P. Ratajczak, A. M. Shah et al., "Increased neuronal nitric oxide synthase-derived NO production in the failing human heart," *The Lancet*, vol. 363, no. 9418, pp. 1365–1367, 2004.

[83] K. Y. Xu, D. L. Huso, T. M. Dawson, D. S. Bredt, and L. C. Becker, "Nitric oxide synthase in cardiac sarcoplasmic reticulum," *Proceedings of the National Academy of Sciences of the United States of America*, vol. 96, no. 2, pp. 657–662, 1999.

[84] K. Y. Xu, S. P. Kuppusamy, J. Q. Wang et al., "Nitric oxide protects cardiac sarcolemmal membrane enzyme function and ion active transport against ischemia-induced inactivation," *Journal of Biological Chemistry*, vol. 278, no. 43, pp. 41798–41803, 2003.

[85] N. Burkard, A. G. Rokita, S. G. Kaufmann et al., "Conditional neuronal nitric oxide synthase overexpression impairs myocardial contractility," *Circulation Research*, vol. 100, no. 3, pp. e32–e44, 2007.